



<https://doi.org/10.30678/fjt.112690>

© 2022 The Authors

Open access (CC BY 4.0)

<https://journal.fi/tribologia>

Effects of reinforcement grain size and concentration on the physicommechanical properties of green automotive brakepads from waste cowhorns and rockshells

Chinwuba OSSIA, Caleb Oguzie, Joshua Evuetapha

Mechanical Engineering Department, University of Port Harcourt, Port Harcourt, Nigeria

Corresponding author: Chinwuba OSSIA (chinwuba.ossia@uniport.edu.ng)

ABSTRACT

This study presents the development and characterization of green automotive brakepads using cowhorn (CH) and Rockshell (*Thias Coronata L.*) (R) as reinforcement material in full factorial experiments. The brakepads were produced by compression moulding at 220.73N using epoxy resin binder, CaCO₃ fillers, Diethylenetriamine hardener, colourless methyl-ethyl ketone peroxide (MEKP) catalyst, carbon black friction modifier, with copper and iron fillings as thermal conductivity additives. Three levels of particle grain sizes 125, 250, 500µm were produced from each material. Hybrid CHR samples were also produced with same grain sizes. The density, hardness, and compressive strength properties were observed to reduce with increase in grain size while liquid absorption increased with increase in grain size. Impregnating the reinforcement materials with increasing concentration of R-particles improved the hardness, compressive strength and liquid absorption but decreased the friction coefficient. The R-samples performed best among all in liquid absorption, except for oil absorption where the commercial (control) sample surpassed it. EDX spectroscopy results showed presence of antimony and vanadium toxic heavy metals in the control sample unlike the developed brakepads. All properties measured exhibited multivariate quadratic regression models with good fitness of R²-values, 0.8438 ≤ R² ≤ 0.9976, and significance-F values, 0.000398 ≤ significance F. ≤ 0.18101. All response surfaces showed best performance with R-concentration of 80 – 100% and 125 – 250µm grain size ranges. Hence, reinforcements of cowhorn and rockshell particles with concentration and grain sizes above can be used to develop brakepads with properties superior to the toxic control brakepads.

Keywords: Brakepad, Cowhorn, Grain size, Rockshell

1. Introduction

So much human risks have been reported with the use of asbestos-based materials [1], [2], [3] which resulted in the ban of asbestos-based engineering materials [4] due to its carcinogenic effect. Similarly, Grigoratos and Martini [5] estimates that half of the total brake wear of most commercial brake pads is emitted as airborne particles of diameter 10µm. These dusty emitted wear particles can be harmful to the environment since they are made of potentially hazardous materials [6]. Subsequently, Gunnath and Bijwe [7] conducted research to explore ecofriendly alternatives even in the automotive industry. Other research works have been done with agricultural wastes being used as alternative reinforcement material to produce brakepad linings. Abutu et al. [8] and Ossia et al [9] used coconut shell in producing asbestos-free brakepads. Tests conducted shows that their newly developed brakepad compared favourably with commercially available brakepads.

Akincioglu et al [10] produced asbestos free brakepads from boron oxide (6%) and hazelnut shell (7%) dusts and 17 other components, both brakepads had higher hardness

than commercial brakepad, with hazelnut shell brakepad being the hardest. Both brakepads had higher coefficient of friction than commercial brakepad, with hazelnut shell brakepad being the highest. Hence, hazelnut shell and boron oxide brakepad can be used commercially.

Bala et al [11] produced asbestos free brakepad linings using pulverized cow hooves with epoxy resin, barium sulphate, graphite and aluminium oxide. The hardness, compressive strength, coefficient of friction, water and oil absorption, relative density and wear rate of the brake linings were determined and compared with existing brake lining properties. The test results showed that proper bonding was achieved with an increase in epoxy resin concentration and decrease in pulverized cow hooves concentration. The scholars concluded that pulverized cow hooves can be used as brake lining material for automobiles.

Abutu et al [12] produced asbestos free brakepads using seashell, epoxy resin (binder), graphite (friction modifier) and aluminum oxide (abrasive). Rule of mixture was used for formulation and a weight percent of 52%wt reinforcement, 35%wt binder, 8%wt abrasive and 5%wt friction modifier were used for production. Tests indicate

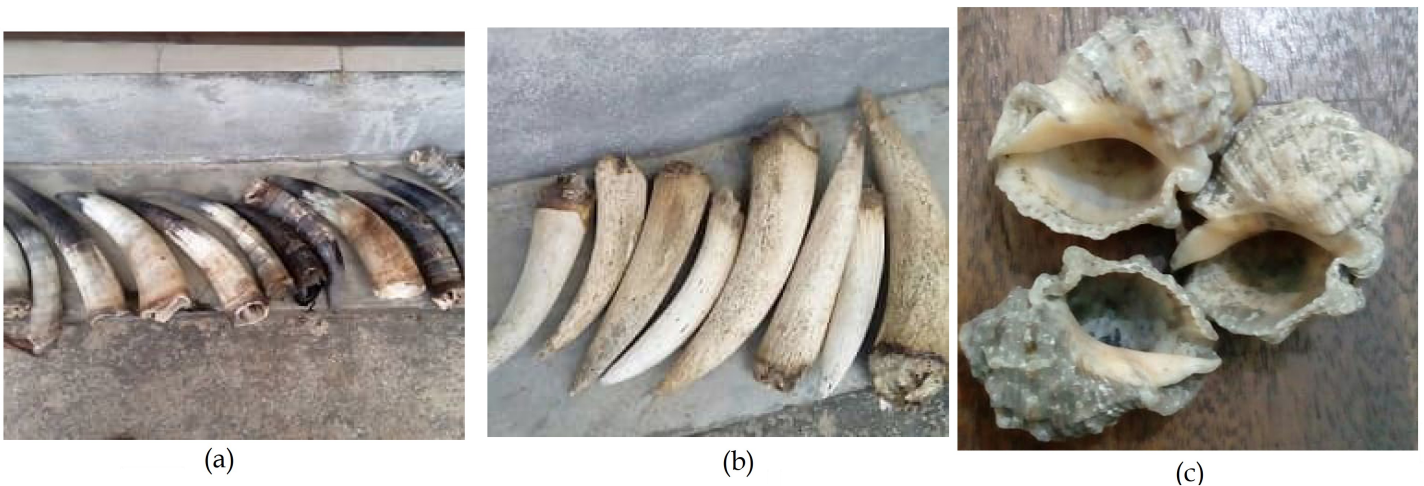


Figure 1: (a) Outer cowhorn (CH), (b) Core cowhorn (CH) and (c) Rockshell (*Thais Coronata L.*) (R) before crushing and grinding



Figure 2: Cow Horn in (a) Crushed and (b) Grinded conditions

that optimum performance can be achieved with 14MPa moulding pressure, 160°C moulding temperature, 12min curing time and 1h heat treatment time. The brakepad had better friction coefficient than commercial brakepads and compares favourably with commercially available brakepads.

Amaren et al [13] studied the effect of grain size on periwinkle shell developed brakepad for different particle sizes between 125 μ m to 710 μ m using phenolic resin as the binder. The 125 μ m particles of periwinkles gave the best wear resistance. The results of this research indicate that periwinkle shell particles can be effectively used as a replacement for asbestos in brakepad manufacture.

Idris [14] used banana peel to produced asbestos free brakepad, with Phenolic resin as binder. The resin was varied from 5 to 30% with interval of 5%. Morphology, physical, mechanical and wear properties of the brakepad were studied. The compressive strength, hardness and specific gravity of the produced samples were observed to be increasing with increase in %wt resin addition, while the oil soak, water soak, wear rate and percentage charred decreased as %wt of resin increases. The samples, containing 25%wt in uncarbonized banana peels and 30%

wt carbonized gave the better properties in all. The result of this research indicates that banana peels particles can be effectively used as a replacement for asbestos in brakepad manufacture.

Nwigbo and Asogwa [15] developed asbestos free brakepads using Rice Husk and Palm Kernel Shell powder as a major constituent in the mix of other regular ingredients in the brakepad manufacture. In this experimental study, the average changes of friction surface, amount of wear loss, stopping time or deceleration, oil and water absorption, hardness capacity of the pad and the noise level generated of sample one (S1) at contact air pressure of 15kN compares relatively well with that of commercial brakepad.

Elakhame et al [16] developed brakepad using palm kernel shell for grain sizes of 100 μ m, 350 μ m, 710 μ m and 1000 μ m. The brakepad were developed by compression moulding using 20% resin, 10% graphite, 15% steel, 35-55% palm kernel shell and 0-20% SiC. The properties examined are microstructure analysis, hardness, compressive strength, density, flame resistance, water and oil absorption. The microstructure reveals uniform distribution of resin in palm kernel shell. The results

obtained showed that the finer the grain size the better the properties which compares favourably with that of commercial brakepad.

This study investigates the tribological performance of ecofriendly brakepads developed from waste Rockshells (*Thais Coronata L.*) and waste cowhorns by: (a) determining the effect of grain size and concentration of these reinforcement materials on the physicochemical and tribological properties of the developed brakepads; and (b) comparing these properties of the developed brakepads with those of a control (commercially available) brakepad.

2. Materials and Methods

2.1 Materials and Equipment

The materials used for the sample preparation includes: (a) cowhorn (CH) fibre reinforcement, (b) Rockshell (R) reinforcement, (c) Calcium carbonate (CaCO_3) fillers, (d) Diethylenetriamine Hardner, (e) Colourless methyl-ethyl ketone peroxide (MEKP) catalyst, (f) Epoxy resin binder, and (g) Carbon black friction modifier. Laboratory equipment used for sample preparation include sieves of various sizes (BS 410 Standard sieves), electric oven (model: GE30, UK), electronic weighing balances (model: ECB600, Germany), circular mild steel moulds, and SAE 40 oil (Oando).

2.2 Sample Preparation

Cowhorn (CH) fibre was extracted from the CH core and the outer CH was discarded, the CH fibre was washed and sun dried for 5 days after which it was crushed and grinded into powdered form. It was then sieved to 125, 250 and 500 μm . The same process was repeated for Rockshell (*Thais Coronata L.*) reinforcement material. The CaCO_3 filler, carbon black friction modifier, copper fillings, iron fillings and sieved pulverized CH and sieved pulverized Rockshell (*Thais Coronata*) were measured according to Table 1 and mixed in a plastic basin to obtain a homogeneous composite. Then epoxy resin, MEKP catalyst, and diethylenetriamine hardener were thoroughly mixed in separate beakers before adding and mixing them with the homogeneous composite. The final homogeneous mixture was transferred to the mould cavity for compression moulding with 220.725N load and allowed to set for 90min minimum duration. The samples were cured by heating in an electric oven at 165 $^\circ\text{C}$ for 4h to improve hardness. The post-cured samples were kept in a ventilated environment for a minimum of 7 days before testing.

2.3 Brakepad development Process

The Brakepad samples were moulded according to the composition in Table 1 through the preparation process shown in Figure 3. Typical moulded samples were exposed to the atmospheric temperature, pressure and humidity for minimum of 7 days as post-curing treatment before machining and testing.

Table 1: Composition of brakepad samples

S/No	Material	Composition (%wt)		
		CH Samples	CHR Samples	R Samples
1	Cowhorn	54.7	27.35	0
2	Rockshell	0.0	27.35	54.7
3	Calcium Carbonate	9.7	9.7	9.7
4	Copper fillings	1.3	1.3	1.3
5	Iron fillings	1.0	1.0	1.0
6	Carbon black	0.5	0.5	0.5
7	Epoxy Resin	20.0	20.0	20.0
8	Hardener	10.0	10.0	10.0
9	MEKP	2.8	2.8	2.8

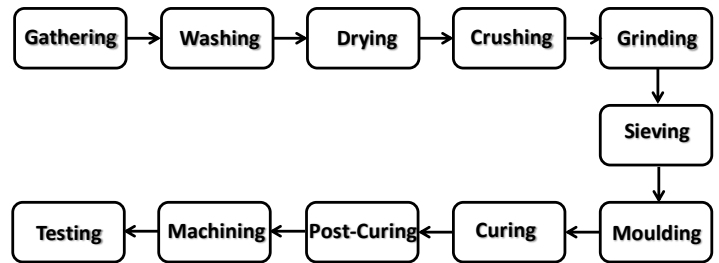


Figure 3: Sample Preparation Process

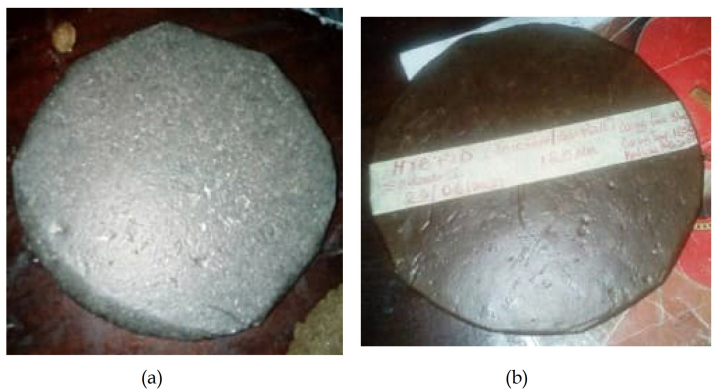


Figure 4: Moulded CHR125 samples (a) before, and (b) after curing at 165 $^\circ\text{C}$ for 4h

2.4 Sample Testing

All the physicochemical and tribological tests were performed based on a 3 levels 2 factors (3^2) full factorial design of experiments with the test-runs as shown in Table 2. The independent (input) variables were rated -1, 0 and 1 to reduce the effect of variable weights.

Rockshell material concentration factor X_1 levels were: -1 (0%R, 100%CH), 0 (50%R, 50%CH), and 1 (100%R, 0% CH) whereas grain size factor X_2 levels were: -1 (125 μm), 0 (250 μm), and 1 (500 μm). Hence, sample ID CH125 describes a specimen with 0% Rockshell 100% CH as reinforcement all sieved to 125 μm grain size (ie, $X_1 = -1$, $X_2 = -1$), CHR250 describes a specimen with 50% Rockshell 50% CH as reinforcement all sieved to 250 μm grain size (ie, $X_1 = 0$, $X_2 = 0$); CHR500 describes a specimen with 50% Rockshell 50% CH as reinforcement all sieved to 500 μm grain size (ie, $X_1 = 0$, $X_2 = 1$) and R500 describes a specimen with 100% Rockshell 0% CH as reinforcement all sieved to 500 μm grain size (ie, $X_1 = 1$, $X_2 = 1$), and so on as

shown in Table 2. The results of the different test properties were reported as output responses (outcomes) in Table 2.

2.4.1 Liquid Absorption Test

Three samples of dimension 35mm by 35mm by 5mm were cut out of the moulded samples and used for the water, boiling water and oil absorption test. The dry weight of each sample was measured and recorded as before immersing in water and Oando SAE 40 oil for 24h. For the boiling water test, the samples were placed in boiling water for 2h. At the expiration of that time, the samples were brought out of the absorbent medium and thoroughly cleaned. The new weight of the sample was then recorded as . The percentage of absorption of the samples was obtained using the following Equation (1).

$$Absorption (\%) = \frac{W_1 - W_0}{W_s} * 100 \quad (1)$$

2.4.2 Density Test

The density of the brakepad samples were obtained by dividing the mass of the sample by the volume as in equation (2). The volumes of the samples were obtained by applying Archimedes' principle of displaced volume, the mass was obtained by weighing the samples on a balance [10], [16].

$$Density = \frac{Mass}{Volume} \quad (2)$$

2.4.3 Compression Test

A Universal Testing Machine (model: UTM-3000, Germany) was used to determine the compressive strength of the samples. A sample was firmly held on the compression plates between the adjustable and bottom cross-heads. When load is applied, the output display unit shows the corresponding strain value, which was taken at regular intervals. The final value was recorded just before the sample failed.

2.4.4 Hardness Test

A mobile hardness Tester was used in testing the hardness of each samples, the 3 tests was done on random

points on each sample and the average on the Brinell hardness scale was recorded as the hardness of that sample

2.4.5 Energy Dispersive X-Ray (EDX) fluorescence Spectroscopy Test

An X-MET7500 was used in this Test. The X-MET7500 was placed on each sample, the trigger pulled and held firmly, the indicator turns yellow showing that the X-ray is on and the machine is identifying the sample after the measurement time the machine make a ping sound, the trigger was released and the readings displayed.

2.4.6 Friction and Wear Test

A pin-on-disc tribometer was used to evaluate the friction and wear properties of the brakepad samples. The samples were machined into a cylindrical pin of 12mm diameter by 10mm height, and loaded with an 8N force against a disc which was rotated to produce a constant interfacial sliding speed of 10cm/s for 507s duration and sliding distance of 50m. The mass of each sample were measured and recorded before and after the tribotesting to obtain the wear rate, while the friction history was recorded as the interfacial rubbing continued within the experimental period.

2.4.7 Optical Micrograph

Snapshot of an optical microscope were taken from the samples before and after the test on the pin on disc apparatus, this is done to get the wear tract. This gives a magnifying image of the samples before and after tribotesting.

3. Results and Discussion

Based on different experimental runs of the design of experiment the test results are shown in Table 2

3.1 Liquid Absorption

The result of the liquid absorption tests for the brakepad samples are shown in Figure 5. All the brakepad samples showed greater absorption in the hot water test than cold water and oil absorption tests. This is due to the expansion of the samples due to temperature rise with consequent expansion of pores making them to absorb

Table 2: Three levels two factors (32) full factorial experimental responses

S/N	Sample ID	Conc. factor, X ₁	Size factor, X ₂	Density, g/cm ³	Absorption, %			Hardness, BHN	CS, MPa	COF
					Oil	Cold water	Hot water			
1	CH125	-1	-1	1.460	1.25	9.13	19.28	144	8.7714	0.643
2	CH250	-1	0	1.294	7.69	18.35	24.69	142	7.6771	0.609
3	CH500	-1	1	1.075	16.83	23.38	33.87	100	4.7429	0.606
4	CHR125	0	-1	1.791	0.92	3.58	5.83	181	11.5143	0.577
5	CHR250	0	0	1.551	0.96	3.73	7.33	178	9.8759	0.564
6	CHR500	0	1	1.431	18.38	12.66	24.76	176	7.6857	0.54
7	R125	1	-1	2.121	1.4	0.70	4.93	242	14.2572	0.511
8	R250	1	0	1.808	1.76	0.65	4.25	236	12.908	0.477
9	R500	1	1	1.789	1.08	0.70	3.61	234	10.8287	0.474

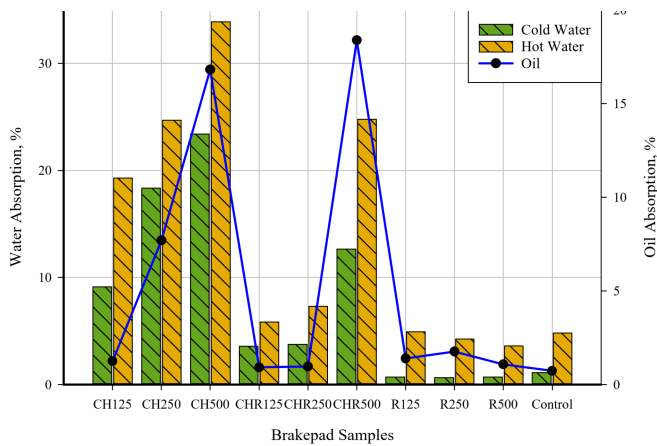


Figure 5: Liquid absorption of the developed and control brakepad samples

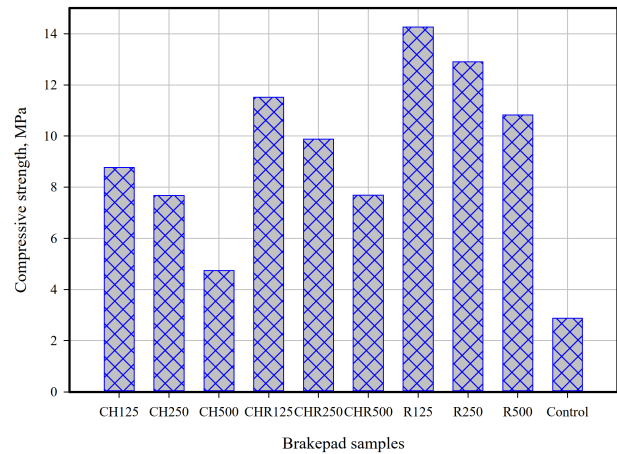


Figure 7: Compressive strength of developed and control brakepad samples

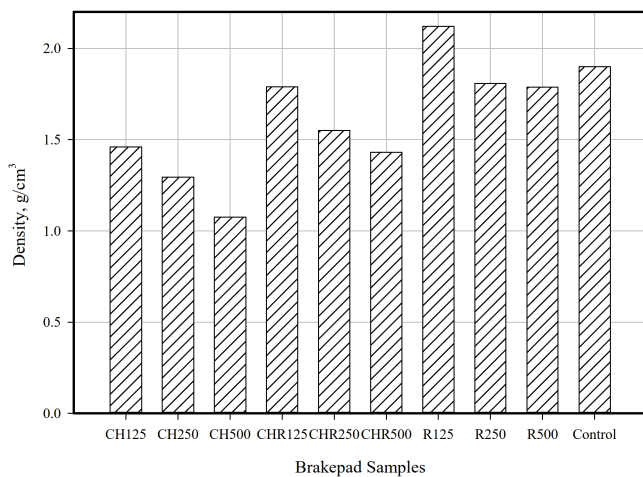


Figure 6: Density of the developed and control brakepad samples

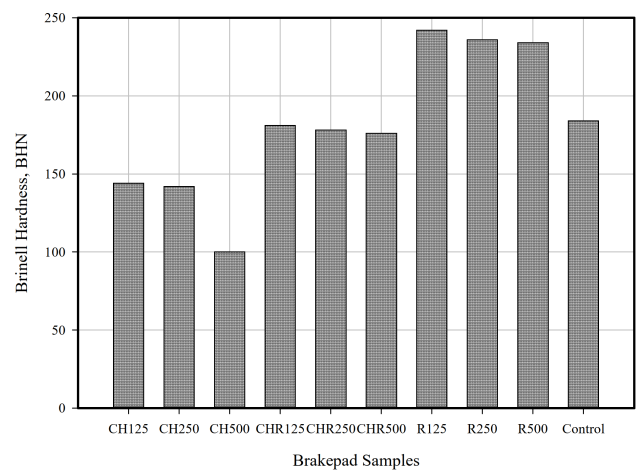


Figure 8: Hardness of the developed brakepad and control sample

more water. The liquid absorption characteristics of the brakepad samples followed the order CH-samples > CHR-samples > R-samples. The liquid absorption property of the R-samples was observed to be comparable to that of the control brakepad sample. This absorption trend is corroborated by the results of Ibadode and Dagwa [17] though their work was based on palm kernel shell. Their study showed that the increase in absorption (swelling) was due to (a) bulging of hygroscopic elements and (b) the release of compression stresses imparted to the brakepad during pressing (springback phenomenon). The control-sample better performance in liquid absorption than CH and Hybrid CHR-samples can be attributed to finer grain size particles giving rise to smaller pores as in the R-samples.

3.2 Density Test

The density test results in Figure 6 show that the developed brakepad densities followed the order CH-sample < CHR-samples < R-samples. R-samples density was comparable with the control-sample density. Furthermore, the density also reduced with increase in grain sizes for all samples. This implies that the control

sample was heavier than the CH-samples and Hybrid CHR-samples which gives the CH-samples and Hybrid CHR-samples advantage of lightness.

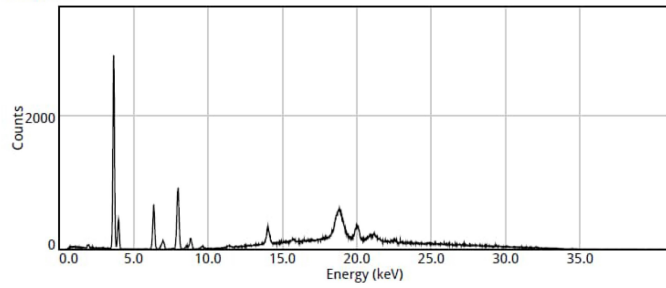
3.3 Compressive Strength

Figure 7 shows that the compressive strength of all CH-samples, Hybrid CHR-samples and R-samples brakepad decrease with increase in grain size; and all the developed brakepad samples exhibited superior compressive strength compared to the control-sample. As the grain size increases, the strength of the interfacial bonding decreases and the nucleation sites for mechanical failure multiply. Hence, the samples with larger grain sizes fail at lower compressive loads due to the combined effect of weaker bonding and more crack initiation and propagation sites. The developed brakepad compressive strength followed the order of CH-sample < CHR-samples < R-samples due to the fibrous nature of cowhorn particles as compared to Rockshell (R).

3.4 Hardness Test

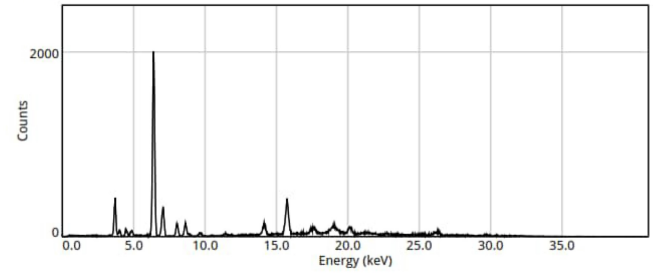
Figure 8 shows the results of the hardness tests carried out on the brakepad samples. The CH-samples, Hybrid

Name	Class		Date	Time	Duration				
JOSHUA A	alloy_fp		14/08/2021	11:43:33	15.5 s				
Element	Fe %	Co %	Cu %	Zn %	Zr %	Nb %	Pd %	W %	Au %
±	32.03	2.12	46.98	1.84	0.94	0.71	12.03	0.69	2.65
Reference:	0.454	0.139	0.527	0.100	0.190	0.207	0.924	0.151	0.237



(a) CH125 sample

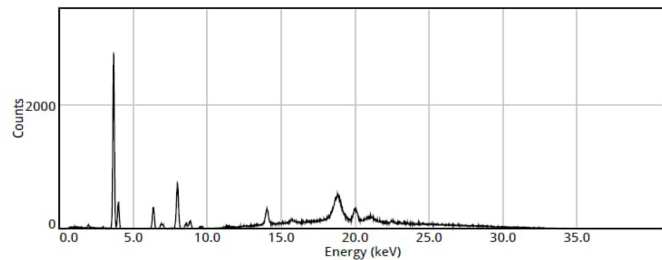
Name	Class		Date	Time	Duration					
Joshua X	alloy_fp		30/04/2021	12:01:50	15.5 s					
Element	Fe %	Sb %	Ti %	Cu %	Zr %	Zn %	V %	Sn %	Pd %	Mo %
±	71.23	7.00	6.44	4.35	3.98	3.33	1.69	0.86	0.61	0.50
Reference:	0.544	0.377	0.382	0.156	0.068	0.122	0.463	0.241	0.121	0.046



(e) Control sample

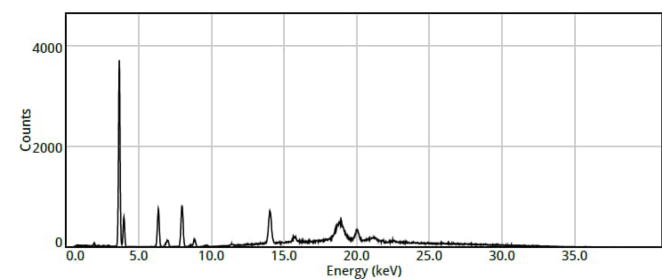
Figure 9: EDX spectroscopy results for: (a) – (d) developed brakepad samples, and (e) Control sample

Name	Class		Date	Time	Duration			
JOSHUA D	alloy_fp		14/08/2021	11:46:39	15.5 s			
Element	Fe %	Co %	Cu %	Zn %	Zr %	Nb %	Pd %	Au %
±	24.80	3.01	46.97	4.66	1.62	0.83	14.66	3.46
Reference:	0.480	0.182	0.604	0.180	0.251	0.271	1.255	0.336



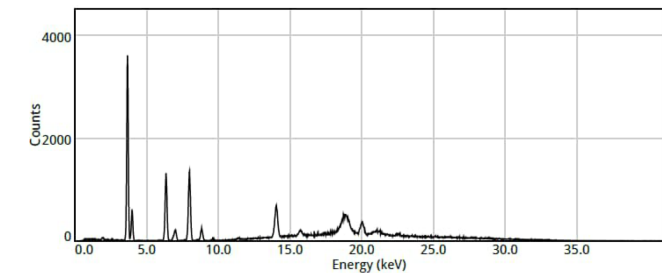
(b) CH500 sample

Name	Class		Date	Time	Duration			
JOSHUA G	alloy_fp		14/08/2021	11:49:56	15.5 s			
Element	Fe %	Co %	Cu %	Zn %	Zr %	Hf %	Au %	
±	36.44	2.15	43.69	1.39	3.01	9.46	1.26	2.61
Reference:	0.487	0.143	0.526	0.097	0.193	0.872	0.406	0.245



(c) CHR250 sample

Name	Class		Date	Time	Duration			
JOSHUA H	alloy_fp		14/08/2021	11:50:38	15.5 s			
Element	Fe %	Co %	Cu %	Zn %	Zr %	W %	Au %	
±	40.27	1.65	46.73	0.57	1.97	6.72	0.21	1.88
Reference:	0.402	0.102	0.449	0.053	0.132	0.574	0.098	0.170



(d) CHR500 sample

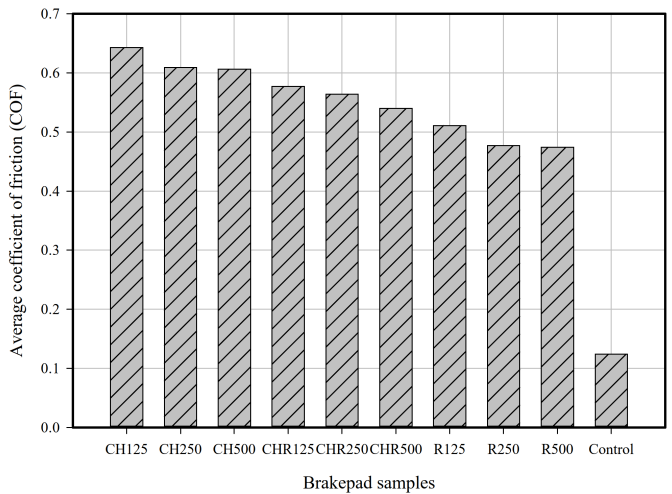
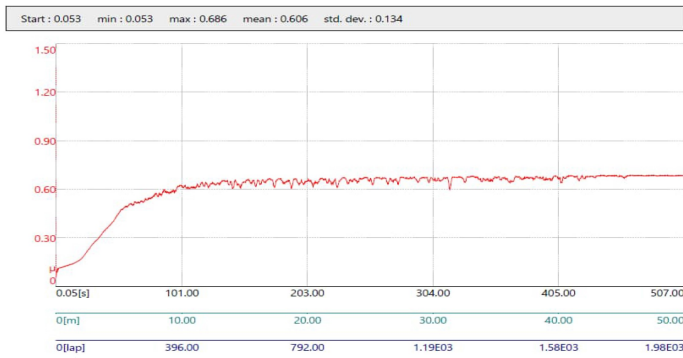


Figure 10: Average coefficient of friction (COF) of brakepad samples

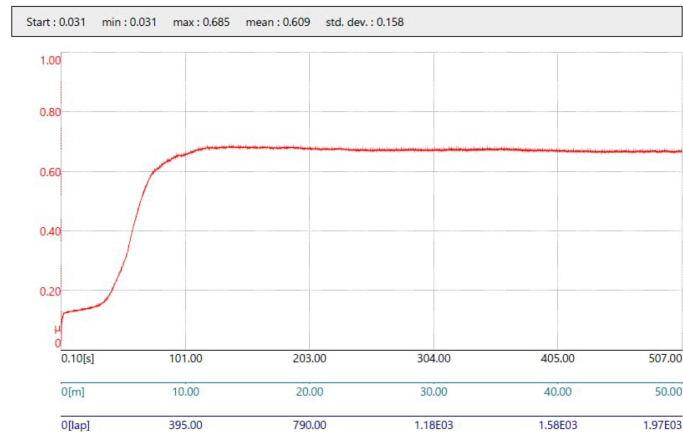
CHR-samples and R-samples hardness decreased with increase in grain size because the particles bonded less compactly due to the increased pore sizes associated with grain size increase. The R-samples were harder than the hybrid CHR-samples which were in-turn harder than the CH-samples. The R-samples hardness was more than the control but the later was comparable to CHR-sample hardness and more than CH-sample because Rockshell improved the hardness of the Cowhorn due to greater cohesive bonding of its particles.

3.5 Energy Dispersive X-Ray Fluorescence Spectroscopy

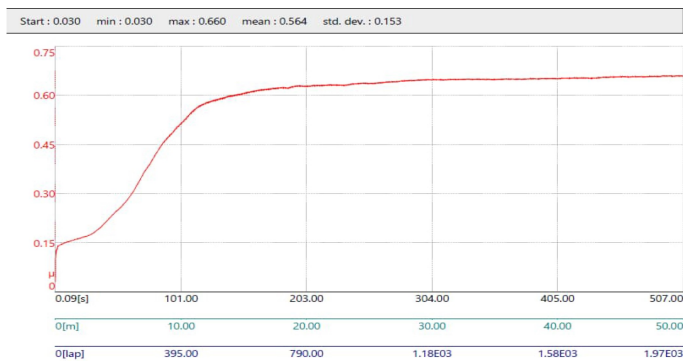
The results from the energy dispersive x-ray (EDX) spectroscopy tests shows that the control-sample brakepad had more toxic heavy metals than the developed organic CH-samples, CHR-samples and R-samples brakepads. The antimony Sb (7%) and vanadium V (1.69%) and tin Sn (0.86%) which were found in the control-samples (Figure 9e) have been reported to be toxic heavy metals / non-essential metals and have been reported to have no established biological functions in human bodies [18], [19]. Iron Fe (24.8 – 40.27%), copper Cu (43.69 – 46.98%) and



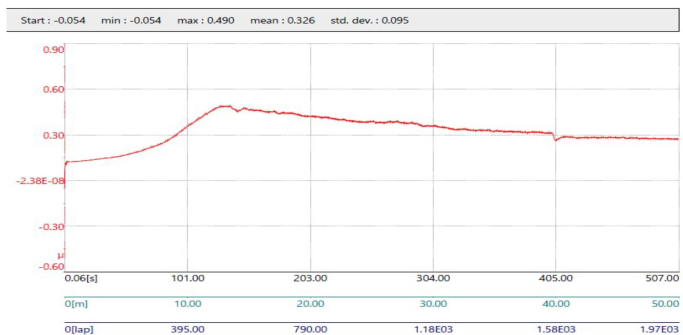
(a) CH125 sample



(b) CH500 sample

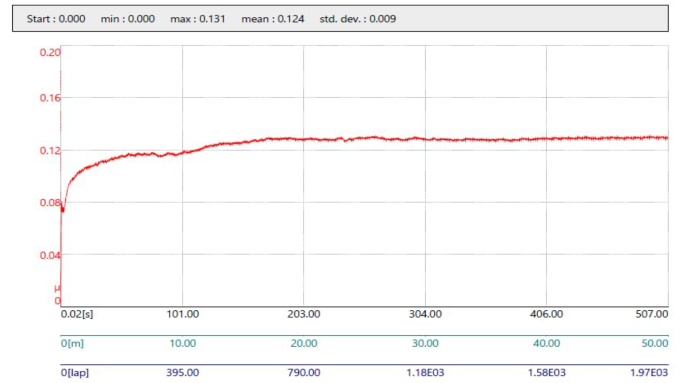


(c) CHR125 sample



(d) CHR500 sample

cobalt Co (1.65 – 3.01%) found in the developed brakepads (Figures 9a – 9d) are heavy metals classified as essential



(e) Control sample

Figure 11: Friction signatures for: (a) – (d) developed brakepad samples, and (e) Control Sample

nutrients which are beneficial and relatively harmless to human [19]. The Cu and Fe in the developed brakepad samples EDX spectroscopy are part of the compounds in Table 1 added during the development process to enhance thermal conductivity. However, palladium pd (6.72 – 14.66%) and Gold Au (1.88 – 3.46%) are quite inert and of low toxicity, being poorly adsorbed by the body when ingested.

3.6 Tribological Tests

Figure 10 shows the average coefficient of friction for the brakepad samples rubbing on steel disc of the pin-on-disc tribometer. It can be observed that the CH-sample brakepads had the highest COF and hence best frictional performance; impregnating the CH-samples with Rockshell reduced the COF-values. This implies that the braking performance of the developed organic brakepads is superior to that of the control-sample brakepad.

The friction histories (signatures) of brakepad sample material rubbing on the steel disc interface are shown in the Figure 11a- Figure 11e. Figure 11a, 11b, 11c, 11d and 11e shows the friction history for CH125-sample, CH500-sample, CHR125-sample, CHR500-sample and control-sample respectively, which are stable at steady-state rubbing condition but Figure 11d showed a healing effect due to wear particle back-filling of pores at the later stage of the friction contact. This healing phenomenon is due to increase in pores and pore sizes as already worn particles stick to the pores acting as lubricant and the pin slides through the already worn particle reducing the friction. This phenomenon was not observed with CH500-sample because of the fibrous nature of the cowhorn particles.

3.7 Optical Micrograph

The optical Micrographs of tribological interfaces (a) before - on the left, and (b) after wear - on the right, are shown in Figures 12(i) – (v). Greater CaCO₃ coagulants can be visibly observed on the Hybrid CHR samples as white spots because Rockshell (R) has high amount of CaCO₃. These coagulants are also observable as fine scattered particles on the CH samples but they are smaller, because

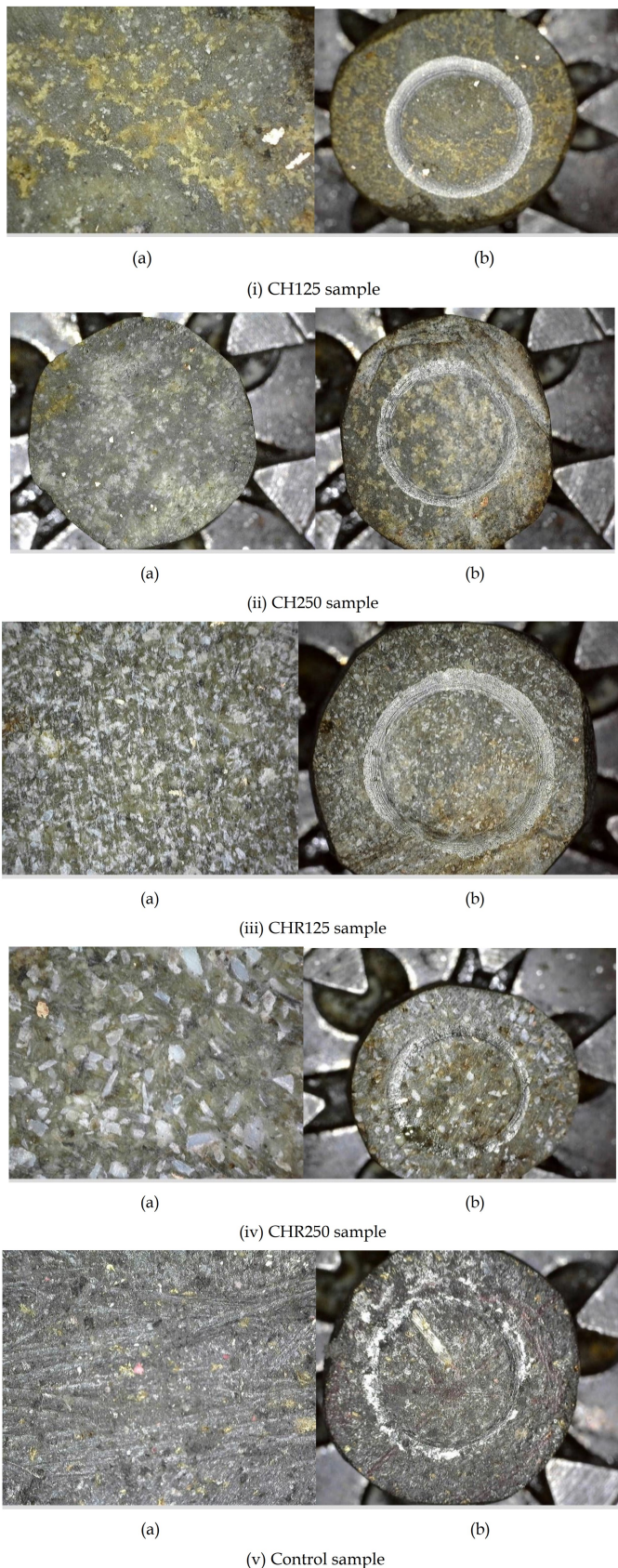


Figure 12: Micrographs of disc interfaces (a) before and (b) after wear for: (i) – (iv) developed brakepad samples and (v) Control sample

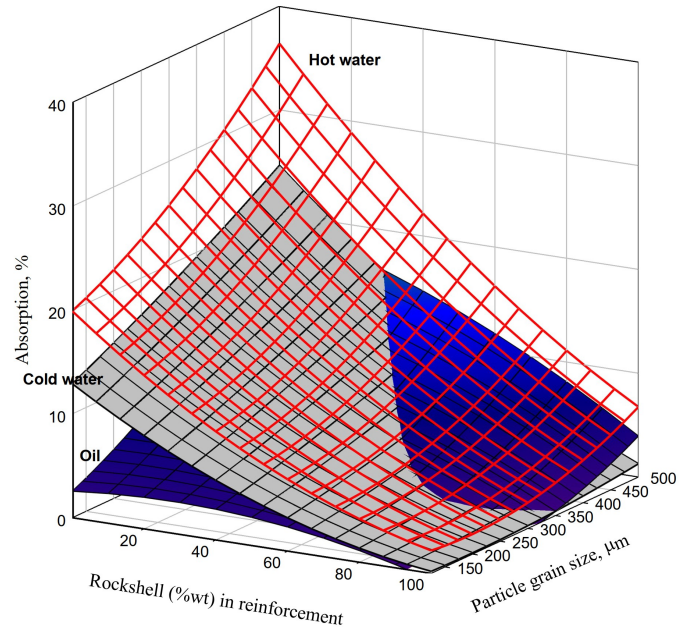


Figure 13: Absorption response of brakepads in hot water (red), cold water (gray) and Oil (coloured)

of the low amount of CaCO_3 filler (9.7%wt) added as in Table 1 as filler.

3.8 Response Surface models

Based on the output of the experimental runs using the 3 levels 2 factors (3^2) full factorial design in Table 2 the different properties were modeled by multivariate regression to obtain the response equations shown in column 3 of Table 3. The coefficients of determination R^2 -values ($0.8438 \leq R^2 \leq 0.9976$) with other statistical parameters obtained in Table 3 showed good fitness of the multivariate regressions models.

The positive quadratic effect of cold water absorption response compared to the positive value for oil absorption model accounts for the coloured bulge in the response surface in Figure 13. It can be observed that the hot water absorption overlaid the cold water absorption surface, which in turn overlaid the oil absorption surface (except for the coloured bulge region highlighted above). The sharp rise in hot water absorption of samples with low Rockshell concentration and high particle grain size is significant because of the effect of intense frictional heating of such brakepads samples in wet environment (arising from spontaneous emergency braking action during rainfall).

Expectedly, the density, compressive strength and hardness of the developed brakepad samples increased with increase in Rockshell concentration (positive main effect) but decreased with particle grain size of the reinforcement (negative main effect) from Figure 14a, Figure 14b and Figure 14c, respectively and Table 3. This is attributable to the observed fibrous nature of the grinded CH compared to the powdery nature of the grinded Rockshell reinforcement-material. Hence, the Rockshell particles helped to stabilize the fibrous cowhorn in the

Table 3: Response surface models of different evaluation properties

Property	Response Model	R ² -value	Std Error	Signif. F.
1 Absorption - Oil	$A_o = 4.6408 - 3.5853X_1 + 5.4502X_2 - 3.9729X_1X_2 - 1.7565X_1^2 + 3.1701X_2^2$	0.8438	4.6126	0.18101
2 Absorption - Cold water	$A_{CW} = 6.1361 - 8.1356X_1 + 3.8890X_2 - 3.5626X_1X_2 + 2.1593X_1^2 + 0.7831X_2^2$	0.9720	2.2954	0.01549
3 Absorption - Hot water	$A_{HW} = 10.4456 - 10.842X_1 + 5.3664X_2 - 3.9768X_1X_2 + 2.4641X_1^2 + 3.2935X_2^2$	0.9300	4.9469	0.058979
4 Density	$D = 1.5507 + 0.3147X_1 - 0.1797X_2 + 0.01315X_1X_2 + 5.4E(-17)X_1^2 + 0.0603X_2^2$	0.9876	0.2350	0.000398
5 Compressive strength	$CS = 10.0388 + 2.8004X_1 - 1.8809X_2 + 0.15X_1X_2 + 0.1723X_1^2 - 0.5203X_2^2$	0.9976	0.0578	0.004663
6 Hardness	$BHN = 182.2222 + 54.3333X_1 - 9.5X_2 + 9X_1X_2 + 4.6667X_1^2 - 5.8333X_2^2$	0.9817	10.7772	0.008269
7 Coefficient of friction - average	$COF = 0.5547 - 0.066X_1 - 0.0185X_2 - 1.3E(-18)X_1X_2 - 0.007X_1^2 + 0.0085X_2^2$	0.9932	0.00808	0.001912

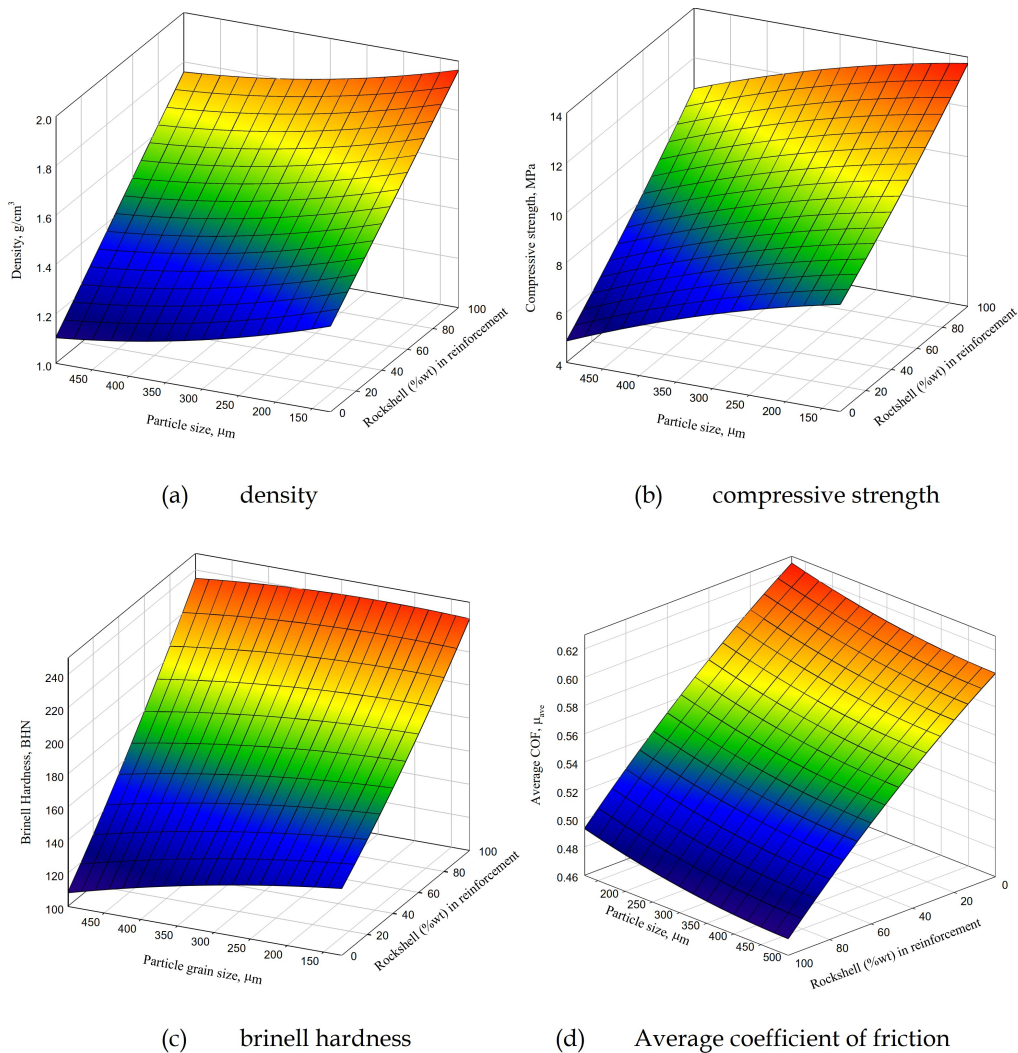


Figure 14: Other brakepads properties response surfaces with respect to particle size and concentration

reinforcement matrix. Higher (particle grain size) aggregates of the samples is associated with larger pores /

voids in the matrix giving rise to lower density, compressive strength and hardness as these pores / voids



Figure 15: Typically finished CHR250 brakepad samples with 250 µm grains Size on backplate

become potential crack nucleation sites since they are stress concentrators. Larger pores / voids will further reduce the critical stress to failure by a power of 2 following crack propagation principles [20]. From Figure 14(d), it can be observed that the average coefficient of friction decreased with increase in particle grain size and increase in rockshell concentration in the reinforcement. This is attributable to the backfilling effect at the pores as the friction phenomenon progresses.

3.9 Finished Hybrid brakepad

The finished hybrid green brakepads with sample ID CHR250 developed by compression moulding using paraffin wax moulds before final back-plating are shown in Figure 15.

4. Conclusion

There was better interfacial bonding between the sample particles and the binder as the particulate grain size decreased. The CH-samples, CHR-samples and R-sample brakepads performed better in compressive strength than the control brakepad, with compressive strength decreasing with corresponding increase in grain size and increase in rockshell concentration in the reinforcement. From the response surface models, the average coefficient of friction decreases with increase in particle grain size and increase in rockshell concentration in the reinforcement. All developed brakepads outperformed the control sample brakepad, with the CH-samples brakepad having the best average coefficient of friction values. The EDX fluorescence spectroscopy result shows that the commercial brakepad contains nonessential and toxic heavy metals like 7% Sb, 1.68% V, 0.86% Sn compared to Fe, Cu, and Co which are classified as beneficial and relatively harmless to humans. Copper (Cu) and Iron (Fe) which were detected in the developed brakepads were added during the development process to

enhance thermal conductivity and stability. The thermal stability of the developed brakepad should be tested, using thermogravimetric analyses (TGA) to ascertain the extent of charring under intense frictional heating arising from spontaneous emergency brake application.

References

- [1] International Agency for Research on Cancer (IARC) (1977), IARC monographs on the evaluation of carcinogenic risks to humans, 14, Asbestos, Lyon: IARC.
- [2] HSE (2009), Health and Safety in Motor Vehicle Repair and Associated Industries, HSG 261, HSE Books, Sudbury, Suffolk.
- [3] Paustenbach D. J, Finley B. L, Lu E. T, Brorby G. P and Sheehan P. J (2010), Environmental And Occupational Health Hazards Associated With The Presence Of Asbestos In Brake Linings and Pads (1900 To Present): A "State-of-the-Art" Review, *Journal of Toxicology and Environmental Health*, 7 (1), pp 25 - 80, <https://doi.org/10.1080/10937400490231494>
- [4] EPA (2018), U.S. federal bans on asbestos, Washington D.C. USA: EPA (accessed 2021 Jul. 30), <http://www.epa.gov/asbestos/us-federal-bans-asbestos>
- [5] Grigoratos T and Martini G (2014), Non-exhaust traffic related emissions: Brake and tyre wear, JRC Science and policy Reports, <https://doi.org/10.2790/21481>
- [6] Peikertova P and Filip P (2016), Influence of the Automotive Brake Wear debris on the Environment- A Review of Recent Research, *SAE International Journal of Material Manufacturing*, 9(1). <https://doi.org/10.4271/2015-01-2663>.
- [7] Gurunath, P. V. and Bijwe, J. (2009), Potential

- exploration of novel green resins and binders for non-asbestos-organic (NAO) friction composites in severe operating condition, *Wear Journal*, 267 (5-8), 789-796. <https://doi.org/10.1016/j.wear.2009.02.012>
- [8] Abutu J, Lawal S. A, Ndaliman M. B, Lafia Araga R. A, Adedipe O, and Choudhury I. A. (2018) Production and characterization of brakepad developed from coconut shell reinforcement material using central composite design, *SN Applied Sciences*, <https://doi.org/10.1007/s42452-018-0084-x>
- [9] Ossia C.V., Big-Alabo A., Ekpruke E.O. (2020) Effect of grain size on the physico-mechanical properties, *Advances in Manufacturing Science and Technology*, 44(4), pp. 135-144, <http://doi.org/10.2478/amst-2019-0023>
- [10] Akincioglu G, Oktem H, Uygur I. and Akincioglu S. (2018), Determination of Friction-Wear Performance and Properties of Eco-Friendly brakepads Reinforced with Hazelnut Shell and Boron Dusts, *Arabian Journal for Science and Engineering*, <https://doi.org/10.1007/s13369-018-3067-8>
- [11] Bala K.C., Okoli M. and Abolarin M. S. (2016), Development of automobile brake lining using pulverized cow hooves, *Leonardo Journal of Sciences*, pp. 95-108, <http://ljs.academicdirect.org/>
- [12] Abutu J, Lawal S. A, Ndaliman M. B, Lafia Araga R. A, Adedipe O, and Choudhury I. A. (2018), Effects of process parameters on the properties of brakepad developed from seashell as reinforcement material using grey relational analysis, *Eng. Sci. Tech., Int. J.* <https://doi.org/10.1016/j.jestch.2018.05.014>
- [13] Amaren, S.G. Yawas, D.S. Aku, S.Y. (2013) Effect of periwinkles shell particle size on the wear behaviour of asbestos free brakepad, *Elsevier*, pp 109-114, <https://doi.org/10.1016/j.rinp.2013.06.004>
- [14] Idris U. D, Aigbodion V. S, Abubakar I.J, Nwoye C.I (2013) Eco-friendly asbestos free brake-pad: Using banana peels, *Journal of King Saud University - Engineering Sciences*, (2015) (27), 185-192, <https://doi.org/10.1016/j.jksues.2013.06.006>
- [15] Nwigbo S. C and Asogwa I. O (2016), Production and performance evaluation of brakepad made from rice husk and palm kernel shell powder. *Inter J Agri Biosci*, 5(6), 391-398, <http://www.ijagbio.com>
- [16] Elakhame Z. U, Alhassan O.A and Samuel A.E (2014), Development and Production of brakepads from Palm Kernel Shell Composites, *International Journal of Scientific & Engineering Research*, 5(10), pp 735 - 744, <http://www.ijser.org>.
- [17] Ibadode A.O.A and Dagwa I.M (2005), Design and manufacture of automobile disk brakepad test rig. *Niger. J. Eng. Res. Dev.*, 4, 15-24.
- [18] Chang, L.W., Magos L., and Suzuki T. (1996); *Toxicology of metals* (eds), CRC Press, USA.
- [19] World Health Organization (WHO) (1996); *Trace elements in human nutrition and health*, World Health Organization, Switzerland, Geneva.
- [20] Peterson, R.C. (2013); *Accurate critical stress intensity factor Griffith crack theory measurements by numerical methods*, *Sample Journal of Society for the Advancement of Materials and Process Engineering*, 2013, 737 - 752.